

Removal of Osteoclast Bone Resorption Products by Transcytosis

Jari Salo,* Petri Lehenkari,* Mika Mulari, Kalervo Metsikkö, H. Kalervo Väänänen†‡

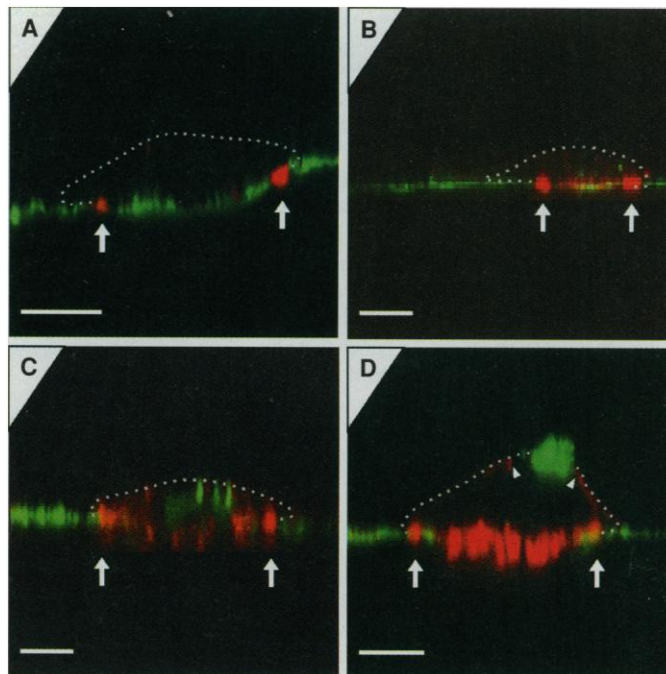
Osteoclasts are multinucleated cells responsible for bone resorption. During the resorption cycle, osteoclasts undergo dramatic changes in their polarity, and resorbing cells reveal four functionally and structurally different membrane domains. Bone degradation products, both organic and inorganic, were endocytosed from the ruffled border membrane. They were then found to be transported in vesicles through the cell to the plasma membrane domain, located in the middle of the basal membrane, where they were liberated into the extracellular space. These results explain how resorbing osteoclasts can simultaneously remove large amounts of matrix degradation products and penetrate into bone.

Bone resorption is an essential component of bone modeling and remodeling during growth and turnover of bone. Disturbances in bone resorption lead to an imbalance in bone metabolism and are behind a large number of metabolic bone diseases, including osteopetrosis and postmenopausal osteoporosis (1–3). During the resorption process, osteoclasts are tightly sealed to the bone surface, and hence the resorption area is isolated from extracellular fluid (4). Osteoclasts dissolve bone mineral by active secretion of protons via vacuolar adenosine triphosphatase through the ruffled border membrane (5). Morphological data show that the degradation of inorganic matrix precedes the degradation of organic matrix, which mostly takes place in extracellular resorption lacunae (6). It has been unclear how osteoclasts handle the large amounts of inorganic and organic material released during the resorption event. Viral glycoproteins that in epithelial cells are targeted to the apical membrane are targeted in resorbing osteoclasts to a specific membrane area in the middle of the basolateral membrane (7). Here we provide evidence that this unusual membrane domain is a target for membrane vesicles that are endocytosed from the ruffled border and contain bone degradation products.

As an experimental model, isolated rat osteoclasts were cultured on bovine bone slices (8). As criteria for a resorbing cell, we used the presence of an actin ring, delineating the resorbing area, or of resorption lacunae as such (9). Various approaches were used to follow the pathway of degradation

products of organic matrix components. We first biotinylated the surface of bovine bone slices on which rat osteoclasts were cultured (10), in order to be able to follow the liberation of organic bone degradation products. Biotinylated proteins were visualized for normal fluorescence and laser scanning confocal microscopy with the use of fluorescein isothiocyanate (FITC)-conjugated streptavidin (green color in Fig. 1). Actin was visualized with tetramethylrhodamine isothiocyanate (TRITC)-conjugated phalloidin (red color in Fig. 1). Using

Fig. 1. Rat osteoclasts were cultured on biotin-labeled bovine bone slices (10) to show the transport of degradation products of organic bone matrix during resorption. (A through D) Osteoclasts in different stages of the resorption cycle, classified on the basis of actin distribution and association to resorption lacuna [for the kinetics and details of the resorption cycle, see (9)]. (A) At the beginning of the resorption cycle, a characteristic ringlike F-actin structure, labeled with TRITC-conjugated phalloidin (red), is formed around the forthcoming resorption area. No biotin (labeled with FITC-streptavidin; green) was observed inside the cell. (B) Some biotin can be seen intracellularly, although most of it is still on the bone surface. (C) A shallow resorption lacuna formed and the biotin label disappeared completely from the bone surface under the osteoclast. (D) Accumulation of biotinylated material at the basal surface of the osteoclast. In the original confocal sections, a discontinuity of cortical F-actin was clearly seen at these gathering sites (gap between arrowheads). Arrows indicate the site of actin rings. Scale bars, 10 μ m.



normal fluorescence microscopy, we found that about 85% of examined resorbing osteoclasts (revealing a distinct actin ring) contained a biotin label. No biotin was seen in nonresorbing cells. With confocal laser scanning microscopy, we first confirmed that nonresorbing cells did not contain the biotin label by scanning through 16 nonresorbing cells. We then scanned 51 resorbing osteoclasts. Four of these resorbing cells showed no biotin inside the cell. In these instances, biotin labeling was intact on the bone surface (Fig. 1A). In most of the scanned resorbing osteoclasts (31 out of 51), the biotin label was observed intracellularly (Fig. 1, B and C). Osteoclasts located over an advanced resorption lacuna (16 out of 51) regularly showed accumulations of biotin in the upper part of the cell (Fig. 1D). This area correlates with the membrane domain (7) that we now consider to be a functional secretory domain. In resorbing osteoclasts, double staining for actin and biotin also revealed a local loss of cortical F-actin in the areas of biotin accumulation (Fig. 1D). This observation is in accordance with results showing local disassembly of the cortical F-actin network during exocytosis in mast cells, chromaffin cells, and pancreatic acinar cells (11).

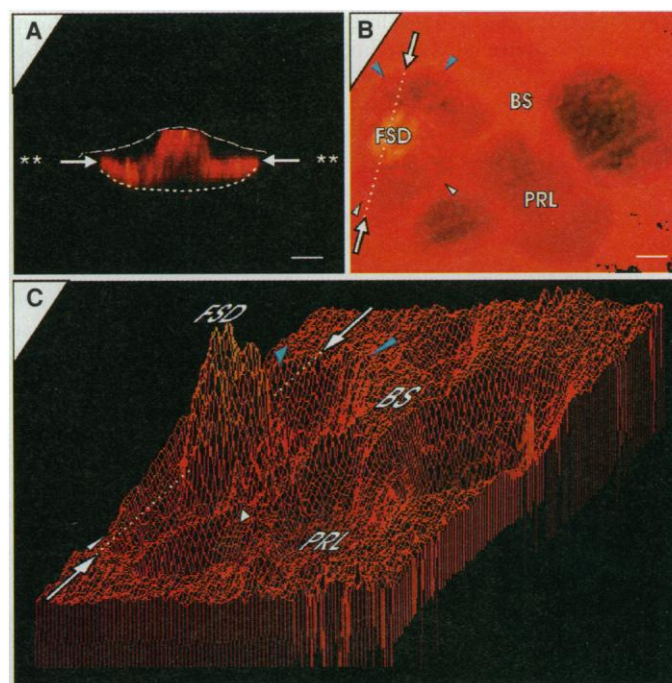
To confirm the results obtained with biotin labeling, we used antibodies to some bone matrix proteins. We used species-spe-

Department of Anatomy and Biocenter, University of Oulu, Kajaanintie 52 A, 90220 Oulu, Finland.

*These authors contributed equally to this work.
†To whom correspondence should be addressed. E-mail: vaananen@raita.oulu.fi

‡Present address: Department of Medical Cell Biology, University of Uppsala, S-75123 Uppsala, Sweden.

Fig. 2. Immunostaining for bovine osteocalcin (12) was seen inside cultured rat osteoclasts and throughout the whole surface of bovine bone slices, including resorption pits. **(A)** A single vertical section from a resorbing osteoclast shows that osteocalcin is seen from the ruffled border area (dotted line) to the topmost part of the cell (dashed line). A typical distribution pattern between these two areas consisted of vesicles forming one or several columnlike structures inside the cell. Only resorbing osteoclasts contained bovine osteocalcin, indicating that osteocalcin was not endocytosed directly from the culture medium, which contained 7% fetal calf serum and degradation products from previous resorption lacunae. Asterisks indicate the surface of the bone slice. In **(A)** through **(C)**, arrows are identically positioned to demonstrate different projections. **(B)** Topographical image of osteocalcin at the resorption site and surroundings. All the original horizontal sections were used for calculation. The color of an individual *xy* pixel is calculated from the center of mass position of staining along the *z* axis. Dark areas indicate that the signal is deep in the sample, whereas bright areas indicate that the signal originates in the upper *xy* planes. In this sample, the bone surface (BS) level is seen in uniform color. Darker areas indicate the walls of the resorption pits, which are below the level of the original bone surface. The bright area on the left shows an osteocalcin signal, which is mostly above the surrounding bone surface. The original *xy* sections of osteocalcin and actin stainings revealed that this staining was located inside the resorbing osteoclast shown in **(A)**. The dashed line indicates the vertical plane for **(A)**. FSD, functional secretory domain; PRL, previous resorption lacuna. **(C)** A pseudo-three-dimensional view is formed from the information in the topographical image. This clearly shows the columnlike shape of the osteocalcin transport route inside osteoclasts. The borders of the actual resorption site are shown by blue and white arrowheads, which also indicate the orientation as compared with **(B)**. Arrows indicate the vertical plane for Fig. 1A. Scale bars in **(A)** and **(B)**, 10 μm .



cific polyclonal antibodies to bovine osteocalcin (12). This antibody does not recognize rat osteocalcin, which means that the

possible presence of endogenous osteocalcin does not interfere with the staining. Bovine osteocalcin (or osteocalcin fragments)

showed a distribution similar to that of biotin-labeled material (Fig. 2), but it was seen throughout the whole transcytotic route. This is probably a result of continuous liberation of osteocalcin fragments from resorption lacunae, compared with the liberation of biotinylated proteins from the surface of the bone. Immunostaining with antibodies to bovine osteonectin (13) revealed similar results.

A transmission electron microscopic study of biotin-labeled bone slices confirmed the observations obtained with immunofluorescence (Fig. 3). An evenly biotinylated bone surface was seen under non-resorbing cells (Fig. 3A), but when there was an apparent local reduction in surface labeling, the biotin label was seen inside the overlying osteoclast (Fig. 3B). In resorbing osteoclasts, the biotin label was in small membranous vesicles from the bone-facing ruffled border to the functional secretory domain (Fig. 3C). In some osteoclasts, biotin-positive vesicles were only in the lower part of the cell, next to the ruffled border. In the functional secretory domain, we regularly observed biotin-labeled material both in the vesicles and as extracellular aggregates in close association with the plasma membrane (Fig. 3D). A small area of plasma membrane also showed biotin labeling (Fig. 3E). This suggests that the transcytotic vesicles containing bone degradation products fuse to the plasma membrane and empty their contents into the extracellular space.

To follow the transport of inorganic material during the resorption process, we labeled bone *in vivo* with sequential injections

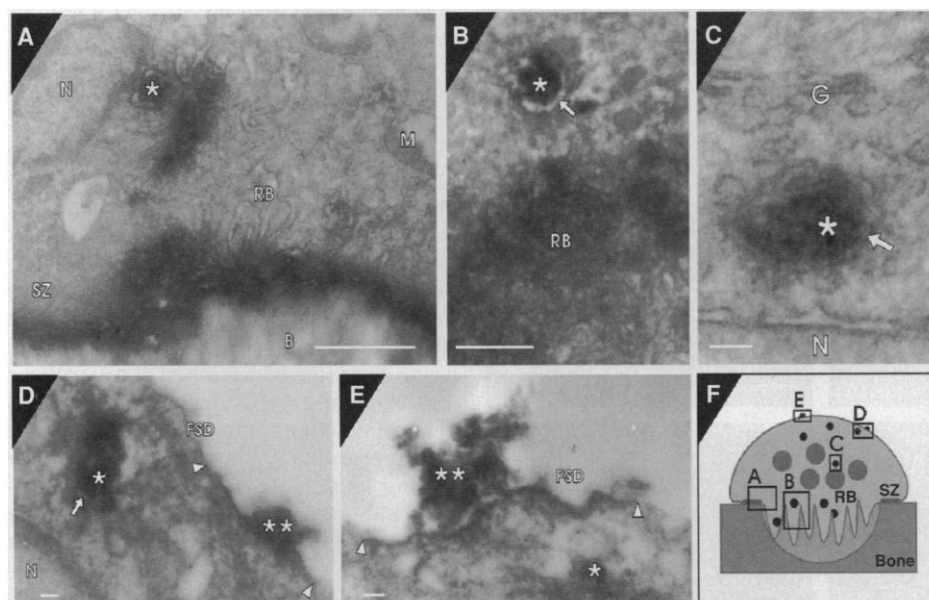


Fig. 3. Transmission electron microscopy (16) of biotin-labeled resorbed bone material. N, nucleus; M, mitochondrion; RB, ruffled border; SZ, sealing zone; B, bone; G, Golgi complex. **(A)** through **(E)** Examples of osteoclasts in different stages of the resorption cycle. **(F)** Sites of panels **(A)** through **(E)**. **(A)** The bone surface (dark band in lower portion of panel) is heavily stained. Some staining is also seen at the ruffled border area, and a single intracellular biotin-containing vesicle (asterisk) is seen. **(B)** In another osteoclast, the ruffled border is heavily stained and more biotin is seen intracellularly. Biotin-containing vesicles regularly showed a light area [arrows in **(B)** through **(D)**] between the vesicle membrane and the biotinylated contents (asterisk). Under this osteoclast, biotin has partly been removed from the surface of the bone slice. **(C)** through **(E)** Osteoclasts with biotin-labeled vesicles (asterisks) throughout the transport route. Resorption lacunae under these osteoclasts had strongly diminished staining or no staining at all for biotin. **(D)** and **(E)** In some osteoclasts, biotin-containing aggregates (double asterisks) were seen extracellularly associated with the plasma membrane. In these areas, the plasma membrane (between arrowheads) also showed local biotinylated. Scale bars in **(A)** through **(E)**, 1 μm .

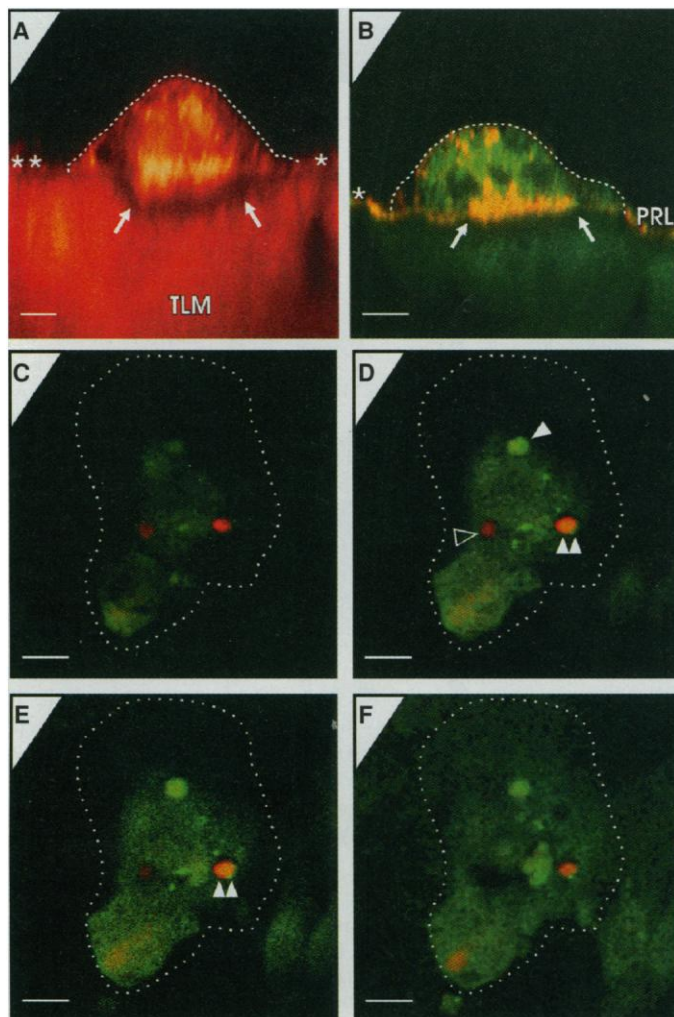
of tetracycline (14). Tetracycline is bound to newly formed mineral and is liberated from the bone matrix when mineral is dissolved before degradation of the organic matrix. On the basis of this process, we hypothesized that during bone resorption, tetracycline is transported along the same route as bone matrix-derived inorganic material. Initial studies indicated that osteoclasts could resorb bone on slices prepared from tetracycline-labeled bone, although tetracyclines have been reported to have some inhibitory effect on bone resorption (15). We applied laser scanning confocal microscopy to follow the appearance and transport of a tetracycline label in cultured osteoclasts (Fig. 4). Cells that were nonpolarized, and not resorbing, did not show intracellular labeling, and the bone slice under them revealed continuous tetracycline labeling. In contrast, oste-

oclasts overlying resorption lacunae were intensively stained (Fig. 4A). A narrow tetracycline-deficient zone just beneath the ruffled border was seen in advanced resorption sites, indicating that mineral had been removed faster than organic matrix was dissolved (Fig. 4A). As in the experiments with biotin labeling, some resorbing osteoclasts showed tetracycline labeling only in the lower part of the cell. Other tetracycline-containing osteoclasts revealed strong labeling all the way up to the basal membrane. However, the label in the upper part of the cell was regularly restricted to the most central part of the basal membrane. To see whether inorganic and organic materials are transported along the same vesicular route, we conducted double labeling experiments, first with tetracycline and wheat germ agglutinin (WGA)-

lectin (Fig. 4B) and second with tetracycline and biotin (Fig. 4, C through F). WGA-lectin is tightly bound to the organic matrix exposed in the resorption lacunae, and during resorption a large number of its binding sites appear intracellularly, especially in the area of the functional secretory domain (7). WGA-lectin binding partly colocalized with tetracycline inside the resorbing osteoclasts (Fig. 4B). We then biotinylated the surfaces of bone slices prepared from tetracycline-labeled bone. Resorbing osteoclasts contained both of these labels (Fig. 4, C through F). The labels were sometimes colocalized but were mostly individually located. We conclude that both organic and inorganic degradation products are taken up and transcytosed along the same route, showing partial colocalization, that was observed with laser scanning confocal microscopy.

We have shown that during bone resorption, osteoclasts endocytose both organic and inorganic degradation products of bone matrix through the ruffled border membrane. Both products are then transported through the resorbing osteoclast, at least partly, in the same population of membranous vesicles. After transcytosis, these vesicles reach the functional secretory domain and empty their contents through this membrane area. Our results offer a solution to a long-standing question in bone biology: How do osteoclasts handle large amounts of degraded bone matrix? They also clarify two other problems involving bone-related disorders. First, it is not known how osteoclasts perform penetrative resorption, which is, for instance, a hallmark of postmenopausal bone loss in aging women. A transcytotic route offers an explanation of how osteoclasts can dig deep resorption channels into compact bone without losing their tight attachment to bone. Second, this route also provides a method of intracellular processing of organic degradation material. This might be an important mechanism in the prevention of autoimmune responses against bone proteins. Finally, earlier characterization of the ruffled border membrane has indicated that it represents either a late endosome- or lysosome-type cellular compartment. Thus, our results offer a new cellular model with which to study vesicular transport from the late endosome- (or lysosome-) type compartment to the cell surface. A transport route between the late endosome-type compartment and the cell membrane also operates during antigen processing before presentation of antigen in various antigen-presenting cells, such as macrophages. Because macrophages and osteoclasts have a common differentiation pathway, it will be interesting to find out if the transport route from late endosome-

Fig. 4. Tetracycline endocytosis and partial colocalization with organic bone matrix material inside osteoclasts. To visualize the inorganic bone matrix, we labeled bone mineral in vivo with oxytetracycline (14). Rat osteoclasts were then cultured on tetracycline-labeled bone slices. (A and B) Cross-sections of two osteoclasts located on resorption lacunae. (A) Tetracycline fluorescence is seen inside the osteoclast and in nonresorbed bone around the resorption lacuna. The label was not present in the resorption lacuna area immediately below the cell (arrows). Asterisks indicate the bone surface. TLM, tetracycline-labeled matrix. (B) Colocalization (yellow) of tetracycline-labeled (green) inorganic matrix material with TRITC-conjugated WGA-lectin (red), which was used to stain intracellular vesicles. The organic surface of tetracycline-labeled bone was also labeled with biotin. Arrows indicate the ruffled border; asterisk indicates the bone surface. (C through F) Tetracycline (green) and biotin (red) were colocalized in several horizontal confocal sections from the top of the cell to the bone surface. In addition to some colocalization (yellow), numerous vesicle-like structures containing either tetracycline or biotin were observed. This could be due to the fact that the biotin label was only on the surface of the bone slice, whereas the tetracycline label was present throughout the whole slice. Tetracycline is indicated by a solid arrowhead, biotin by an open arrowhead, and colocalization by a double arrowhead. Dashed lines indicate the basal surface membrane in (A) and (B) and the periphery of the osteoclast in (C) through (F). Scale bars, 10 μ m.



type resorption lacunae to the cell membrane is in any way analogous to the final antigen-presentation route of macrophages.

REFERENCES AND NOTES

- H. M. Frost, *J. Am. Geriatr. Soc.* **9**, 1078 (1961).
- W. S. Sly, D. Hewett-Emmett, W. P. Whyte, Y. S. L. Lu, R. E. Tashian, *Proc. Natl. Acad. Sci. U.S.A.* **80**, 2752 (1983); H. Yoshida *et al.*, *Nature* **345**, 442 (1990); P. Soriano, C. Montgomery, R. Geske, A. Bradley, *Cell* **64**, 693 (1991); C. Lowe *et al.*, *Proc. Natl. Acad. Sci. U.S.A.* **90**, 4485 (1993).
- G. A. Rodan, L. G. Raisz, J. P. Bilezikian, in *Principles of Bone Biology*, J. P. Bilezikian, L. G. Raisz, G. A. Rodan, Eds. (Academic Press, New York, 1996), pp. 979–990; L. L. Key and W. L. Ries, *ibid.*, pp. 941–950.
- M. E. Holtrop and G. J. King, *Clin. Orthop.* **123**, 177 (1977); H. K. Väänänen and M. Horton, *J. Cell Sci.* **108**, 2729 (1995).
- I. A. Silver, R. J. Murrills, D. J. Etherington, *Exp. Cell Res.* **175**, 266 (1988); H. C. Blair, S. L. Teitelbaum, R. Ghiselli, S. Gluck, *Science* **245**, 855 (1989); H. K. Väänänen *et al.*, *J. Cell Biol.* **111**, 1305 (1990).
- A. Boyde and S. J. Jones, *Scanning Microsc.* **1**, 369 (1987).
- J. J. Salo, K. Metsikkö, H. Palokangas, P. Lehenkari, H. K. Väänänen, *J. Cell Sci.* **109**, 301 (1996).
- A. Boyde, N. N. Ali, S. J. Jones, *Br. Dent. J.* **156**, 216 (1984); T. J. Chambers, P. A. Revell, K. Fuller, N. A. Athanasou, *J. Cell Sci.* **66**, 383 (1984).
- P. T. Lakkakorpi and H. K. Väänänen, *J. Bone Miner. Res.* **6**, 817 (1991); R. T. Lakkakorpi and H. K. Väänänen, *Microscopy Res. Tech.* **33**, 171 (1996).
- Thin bone slices were prepared from the cortex of bovine femurs, incubated in phosphate-buffered saline (PBS) containing water-soluble sulfo-*N*-hydroxysuccinimide-biotin (2 mg/ml) (Pierce, Rockford, IL) for 2 hours, washed repeatedly, and rinsed overnight in PBS. Osteoclast cultures (9) were fixed at 48 hours in 3% paraformaldehyde for 10 min, and cells were permeabilized in 0.5% Triton TX-100. Biotinylated material was visualized with FITC-conjugated streptavidin (Sigma) for 2 hours at room temperature. After extensive washes, samples were incubated in TRITC-labeled phalloidin (Sigma). Samples from eight independent experiments (each containing 18 bone slices with 200 to 300 osteoclasts per slice) were studied with conventional immunofluorescence microscopy. At 48 hours, 63% of the osteoclasts were resorbing and 37% were non-resorbing. Fifty-one resorbing osteoclasts and 16 nonresorbing osteoclasts were scanned with laser scanning confocal microscopy (Leica Aristoplan CLSM, Leica Lasertechnik, Heidelberg, Germany).
- A. Koffer, P. E. Tatham, B. D. Gomperts, *J. Cell Biol.* **111**, 919 (1990); M. L. Vitale, A. Rodriguez del Castillo, L. Tchakarov, J. M. Trifaró, *ibid.* **113**, 1057 (1991); S. Muallem, K. Kwiatkowska, X. Xu, H. L. Yin, *ibid.* **128**, 589 (1995).
- Species-specific polyclonal antibodies (Biogenesis, Poole, England) that recognize bovine but not rat osteocalcin were used (dilution, 1:100, for 60 min at 37°C). Eight independent experiments were performed. Rat osteoclasts were cultured as described for Fig. 1.
- LF-BON-1 antibodies to purified bovine bone osteonectin were a gift from L. W. Fisher, NIH, Bethesda, MD.
- A growing piglet, aged 4 weeks, received daily intramuscular injections of oxytetracycline (Terramycin/LA, Pfizer) at a dose of 20 mg per kilogram of body weight for 6 weeks. After the pig was killed, thin bone slices were prepared from the cortex of the femurs. Approximately one-fourth of the cortical bone area revealed intensive tetracycline fluorescence, whereas the remaining three-fourths served as a negative control. Four independent experiments were performed, and 16 osteoclasts were analyzed in detail with confocal laser scanning microscopy. Rat osteoclasts were cultured on these bone slices (Fig. 1).
- S. Q. Cohan, G. Bevelander, T. Tiamsic, *Am. J. Dis. Child.* **105**, 453 (1963); M. H. Chowdhury, S. A. Moak, B. R. Rifkin, R. A. Greenwald, *Agents Actions* **40**, 124 (1993); B. R. Rifkin, A. T. Verrillo, L. M. Golub, N. S. Ramanurthy, *Ann. N.Y. Acad. Sci.* **732**, 165 (1994).
- Osteoclasts were fixed in 3% paraformaldehyde, permeabilized with saponin, and blocked in 0.1% bovine serum albumin for 15 min. Streptavidin peroxidase (dilution, 1:100) was applied to cells for 60 min. After intensive washes, the 3,3'-diaminobenzidine (0.5 mg/ml) and H₂O₂ (0.6 mg/ml) reaction was carried out. Cells were fixed in 2.5% glutaraldehyde for 90 min at 4°C and osmicated. Bone slices were then decalcified in sodium cacodylate-buffered EDTA (4.13 mg/ml) containing 0.1% glutaraldehyde for 3 days at 4°C, dehydrated, and embedded in Epon LX-112. Thin sections (100 nm) were stained with lead citrate and observed with a transmission electron microscope (Philips 410, at 60 kV). Twenty individual osteoclasts from three independent cultures were analyzed.
- Supported by the Finnish Academy of Sciences and by Astra Hässle AB, Sweden. We thank S. Seinijoki and A. Haimakainen for technical assistance.

12 November 1996; accepted 18 February 1997

Differential Regulation of HIV-1 Fusion Cofactor Expression by CD28 Costimulation of CD4⁺ T Cells

Richard G. Carroll, James L. Riley, Bruce L. Levine, Yu Feng, Sumesh Kaushal, David W. Ritchey, Wendy Bernstein, Owen S. Weislow, Charles R. Brown, Edward A. Berger, Carl H. June,* Daniel C. St. Louis

Activation of CD4⁺ T lymphocytes from human immunodeficiency virus-type 1 (HIV-1)-infected donors with immobilized antibodies to CD3 and CD28 induces a virus-resistant state. This effect is specific for macrophage-tropic HIV-1. Transcripts encoding CXCR4/Fusin, the fusion cofactor used by T cell line-tropic isolates, were abundant in CD3/CD28-stimulated cells, but transcripts encoding CCR5, the fusion cofactor used by macrophage-tropic viruses, were not detectable. Thus, CD3/CD28 costimulation induces an HIV-1-resistant phenotype similar to that seen in some highly exposed and HIV-uninfected individuals.

Infection of CD4⁺ T lymphocytes with HIV-1 is initiated by binding of the viral envelope glycoprotein gp120 to the CD4 receptor on the lymphocyte surface, followed by fusion of the virus with the cell membrane (1). Virus-cell fusion is mediated by members of the chemokine receptor family, with different members serving as fusion cofactors for macrophage-tropic (M-tropic) and T cell line-tropic (TCL-tropic) isolates of HIV-1 (2).

HIV-1 infection is also influenced by the host T cell activation state. Commit-

ment to T cell activation requires T cell receptor (CD3) engagement as well as a costimulatory signal. Interaction of the costimulatory molecule CD28 with its ligands CD80 or CD86 provides a necessary costimulus to induce an immune response (3). In addition to promoting the long-term polyclonal proliferation of CD4⁺ T cells in the absence of exogenous cytokines or feeder cells, activation with immobilized antibodies to CD3 (anti-CD3) and CD28 (anti-CD28) specifically induces a potent anti-HIV effect (4). This resistance is due in part to an enhanced production of the β -chemokines RANTES, MIP-1 α , and MIP-1 β (5), which block infection by M-tropic isolates (6). However, CD3/CD28-stimulated cells express an additional, cis-acting component of resistance specific to costimulation with immobilized anti-CD28 (5). This intrinsic CD3/CD28-specific antiviral effect was examined by comparing the HIV-1 infection process in cells stimulated with either immobilized anti-CD3 and anti-CD28 or with the mitogenic lectin phytohemagglutinin (PHA) and interleukin-2 (IL-2).

Purified CD4⁺ lymphocytes obtained from uninfected donors were cultured either with PHA and IL-2 or with beads coated with the CD3 monoclonal antibody OKT3

R. G. Carroll, S. Kaushal, D. W. Ritchey, D. C. St. Louis, Henry M. Jackson Foundation for the Advancement of Military Medicine, Rockville, MD 20850, USA.

J. L. Riley and W. Bernstein, Division of Retrovirology, Walter Reed Army Institute for Research, Rockville, MD 20850, USA.

B. L. Levine, Immune Cell Biology Program, Naval Medical Research Institute, Bethesda, MD 20889, USA.

Y. Feng and E. A. Berger, Laboratory of Viral Diseases, National Institute of Allergy and Infectious Diseases, National Institutes of Health, Bethesda, MD 20892, USA.

O. S. Weislow, Life Sciences Division, SRA Technologies, Rockville, MD 20850, USA.

C. R. Brown, Laboratory of Infectious Diseases, National Institute of Allergy and Infectious Diseases, National Institutes of Health, Rockville, MD 20852, USA.

C. H. June, Henry M. Jackson Foundation for the Advancement of Military Medicine, Rockville, MD 20850, and Immune Cell Biology Program, Naval Medical Research Institute, Bethesda, MD 20889, USA.

*To whom correspondence should be addressed. E-mail: rin0cxj@bumed30.med.navy.mil